

# Spatiotemporal stochastic resonance and its consequences in neural model systems

Gábor Balázs

*Center for Neurodynamics, University of Missouri, St. Louis, 8001 Natural Bridge Road, St. Louis, Missouri 63121-4499*

László B. Kish

*Department of Materials Science, The Angstrom Laboratory, Uppsala University, P.O. Box 534, Uppsala, SE-75121, Sweden*

Frank E. Moss

*Center for Neurodynamics, University of Missouri, St. Louis, 8001 Natural Bridge Road, St. Louis, Missouri 63121-4499*

(Received 18 December 2000; accepted 4 April 2001; published 31 August 2001)

The realization of spatiotemporal stochastic resonance is studied in a two-dimensional FitzHugh–Nagumo system, and in a one-dimensional system of integrate-and-fire neurons. We show that spatiotemporal stochastic resonance occurs in these neural model systems, independent of the method of modeling. Moreover, the ways of realization are analogous in the two model systems. The biological implications and open questions are discussed. © 2001 American Institute of Physics. [DOI: 10.1063/1.1379042]

**Biological neurons are nonlinear (i.e., threshold) devices. Therefore neural systems are in the focus when looking for realizations of stochastic resonance (SR) or spatiotemporal stochastic resonance (STSR), both of which occur in systems possessing a threshold. There are two different ways to simulate neural systems. The first is based on the FitzHugh–Nagumo (FN) equations, the second is based on a simple integrate-and-fire (IF) model. In this article the effect of noise on neural systems will be discussed using both ways of modeling. The results suggest that SR and STSR do occur in models of neural systems, independent of the model used. This means that an optimal noise intensity can maximize signal transmission through such systems. How significant is the role played by these phenomena and what implications they might have for neurobiology, is still an open question.**

## INTRODUCTION

Stochastic resonance (SR) is a paradox-phenomenon in which an optimal noise intensity maximizes the signal transfer through a nonlinear device.<sup>1–7</sup> A generalization of SR has been introduced recently: spatiotemporal stochastic resonance (STSR). The essence of STSR is that perturbation propagation in extended systems is optimized by noise.<sup>6,8,9</sup>

Excitable media are systems of diffusively coupled nonlinear elements, usually governed by a system of nonlinear partial differential equations. These systems show interesting features, e.g., spiral wave formation and STSR.<sup>10,11</sup>

Spiral waves have been shown to propagate in a variety of systems. Wave propagation in such media is of special interest because it is at the confluence of many “hot” topics; Belousov–Zhabotinsky reactions in chemical systems,<sup>10–13</sup> calcium dynamics in astrocyte cultures,<sup>14</sup> and perturbation

propagation in noisy nonlinear systems.<sup>9</sup> In the following paragraphs, a description of three different excitable media is given, where spiral waves have been observed.

It has been demonstrated<sup>8</sup> that wave propagation in an excitable chemical medium can be supported by noise in the case of the Belousov–Zhabotinsky (BZ) reactions.<sup>12,13</sup> The excitability is governed by the presence of a light-sensitive catalyst for the reaction. Above the threshold the waves are of the reaction-diffusion type. The wave front moves through the medium consuming the BZ catalyst, and leaving in its wake a region of depleted material which is incapable of reaction. The waves have a characteristic shape: that of a propagating single or double spiral. In excitable media, parameters are such that a small disturbance anywhere in the medium results in a wave which propagates out from the disturbed location for an indefinite time and distance. In subexcitable media, however, disturbances do not propagate, but instead die out a short distance/time from the original location.

This picture changes drastically if noise is added to the light intensity. Even in the subexcitable regime, the propagation of waves is supported now by the noise and an optimal noise intensity can result in sustained waves which propagate indefinitely. This is called STSR.<sup>8,9</sup> Figure 1 illustrates this phenomenon, which has also been proven by computer simulations, using a two-dimensional network of elements, governed by the so-called “Oregonator”<sup>15</sup> equations. The elements were coupled to their four nearest neighbors, through diffusive terms added to the following system of differential equations:

$$\frac{du}{dt} = \frac{1}{\epsilon}(qw - uw + u - u^2), \quad (1a)$$



FIG. 1. Images of wave segments traveling through a BZ medium, perturbed by increasing noise intensity starting from 0 and reaching a maximum level permitted by the experiment. (a) No noise; (b) small noise; (c) optimal noise; (d) too strong noise (causing wave fragmentation). [Reproduced from P. Jung, A. Cornell-Bell, F. Moss, S. Kádár, and K. Showalter, *Chaos* **8**, 567–575 (1998), with permission.]

$$\frac{dw}{dt} = \frac{1}{\delta}(\phi - qw - uw + fv), \quad (1b)$$

$$\frac{dv}{dt} = u - v, \quad (1c)$$

where the variables are  $u$ ,  $v$ , and  $w$ ;  $\phi$  is the excitability parameter.

One of the first successful attempts to initiate spiral waves used a neural network.<sup>16,17</sup> Neurons are *threshold elements*, with nonlinear transfer properties as required for SR phenomena. They can be excited through their processes called *dendrites* and transmit the information farther through their axon via impulses called *action potentials*. The excitation takes place by the release of chemicals called *neurotransmitters* in the junctions (*synapses*) between the exciting neuron's axon and the excited neuron's dendrite. The chemicals are stored in small containers called *vesicles* near the end of the axon. When an action potential arrives to the end of an axon,  $\text{Ca}^{2+}$  ions enter through the membrane and cause the release of the neurotransmitter into the synapse. After diffusing through the synaptic cleft, the neurotransmitter binds to the membrane of the excited cell, causing depolarization. The depolarization happens in quanta (in steps), the contribution of each vesicle being approximately equal. The quanta of depolarization are called *excitatory postsynaptic potentials (EPSPs)*. The EPSPs arriving successively from different dendrites within a certain *time constant* specific to the neuron are summed. If the resulting depolarization reaches the threshold, an action potential is generated. After the generation of the action potential the neuron enters an unexcitable state called the *recovery period*.<sup>18</sup>

In the central nervous system besides various types of neurons there are cells responsible for nutrition, control of blood supply, and support called *astrocytes* or *glia*. The astrocytes are similar to neurons from several points of view. First, both types of cells develop from the same original cell in the human fetus. The astrocytes envelop synapses in the brain, and they are depolarized by specific neurotransmitters released by the neurons. If the depolarization reaches a threshold, the astrocytes enter a different state (just like neurons), in which their free  $\text{Ca}^{2+}$  concentration increases abruptly. This causes the increase of the  $\text{Ca}^{2+}$  concentration in the cytoplasm of neighboring astrocytes. It has been discovered recently that this mechanism can also lead to the generation of spiral waves in astrocyte cultures.<sup>14</sup> The spiral waves that were initiated showed similar features to the ones found in the chemical (BZ) system. A quantitative analysis showed self-organized criticality in both cases.<sup>9,19</sup>

The purpose of the present paper is to study STSR in two different (FN and IF) neuron model systems. SR has been shown to be a property of single neurons for both types of models.<sup>20,21</sup> Our results indicate that STSR is also a property of both systems. It is important to mention that while in our FN system the coupling is bidirectional, in the IF system it is only unidirectional. Therefore, the first can model excitable systems in general (and astrocyte cultures in particular), while the latter is mainly suitable to model chains of neurons in peripheral nerves. Nevertheless, the fact that STSR is a property of both systems reveals some deep similarity between general excitable systems and unidirectionally coupled neurons. The implications of the observed phenomena will be outlined in the final section. The paper concludes with open questions.

## FITZHUGH–NAGUMO EQUATIONS

A two-dimensional lattice of elements governed by the FN equations has been considered,

$$\epsilon \frac{dv}{dt} = v(a - v)(v - 1) - w, \quad (2a)$$

$$\frac{dw}{dt} = v - dw - b, \quad (2b)$$

where the variables are  $v$  and  $w$ , while the excitability parameter is  $b$ .  $v$  corresponds to the voltage across the membrane, and  $w$  controls the recovery period. The rest of the

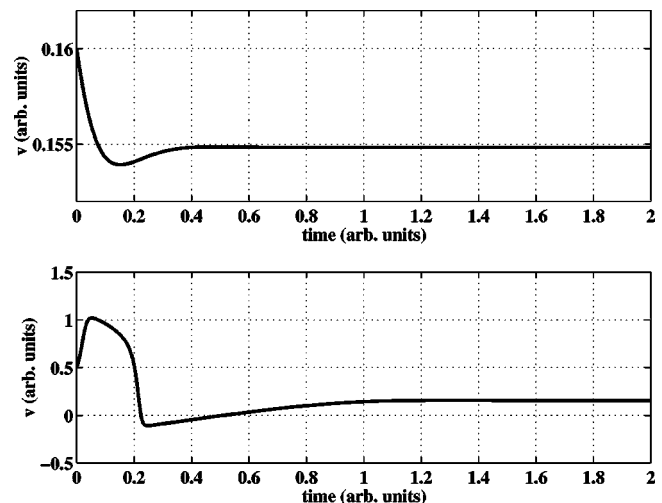


FIG. 2. Solutions of the FN equations in the nonoscillatory regime. (Top) Simple decay to stationary value. (Bottom) Decay to stationary value preceded by one oscillation.



FIG. 3. Spiral wave initiation and propagation.

parameters were kept constant,  $\epsilon=0.005$ ,  $a=0.5$ , and  $d=1.0$ . This pair of equations was originally created to model neuron dynamics.<sup>22,23</sup> Depending on the value of the excitability parameter  $b$  the system has two kinds of solutions. If  $b > 0.26$  the solution is oscillatory (independent of the initial value of  $v$  and  $w$ ). On the other hand, if  $b < 0.26$  the solution decays and reaches a stationary value. The way the stationary value is reached in this regime depends on the initial values of  $v$  and  $w$ . If the initial values are far from the stationary values, the relaxation can happen through an oscillation, consisting of a rapid rise to a maximum, followed by a recovery period. If they are close to the stationary values, the decay is monotonous. The closer we approach the critical value of  $b$ , the less deviation is needed to initiate an oscillation. Very close to the critical  $b$  even damped oscillations can be observed. Therefore the equations inherently contain a threshold. The threshold is the minimum difference from the stationary values for which an oscillation can already be observed. Throughout the following simulations we used the nonoscillating (subexcitable and excitable) regime (see Fig. 2).

If a diffusive term of the form  $\nabla^2 v$  is added to the first equation, the spatial propagation of a perturbation becomes possible. The perturbation propagates as a single or double spiral wave through the medium. Depending on the excitability parameter  $b$ , and the diffusion coefficient  $D$ , the waves are either supported or they vanish after traveling a short distance. Thus, the system can be *subexcitable* (if wave propagation is inhibited) or *excitable* (if wave propagation is supported). The third regime called *hyperexcitable* is characterized by global, synchronized oscillations of all elements, and will not be discussed here. An example of spiral wave propagation is shown in Fig. 3. We generated Fig. 3 as follows: first, a straight wavefront was initiated, by setting the

initial values within a thin vertical area on the right edge of the system above the threshold. The straight wavefront was allowed to propagate freely until both ends of it are cut off. From that time on, the two points where the ends were cut off each became the centers of a spiral.

The medium was chosen to be excitable, with  $b=0.245$ . If the same experiment were repeated in a subexcitable medium (e.g.,  $b=0.2017$ ), spiral wave formation could not be observed; instead, the straight wave segment remaining after cutoff would shrink and disappear completely [see Fig. 4(b)].

If a spatiotemporal noise is added, however, the wave propagation can be sustained even in the subexcitable regime. In Fig. 4 the waves are initiated in an excitable area where  $b$  favors wave propagation ( $b=0.245$ ). Later they enter a subexcitable area, where  $b$  causes wave decay ( $b=0.2017$ ). The diffusion coefficient was defined such that  $D/\Delta x^2 \Delta t=64$ . The images were created by overlaying phases of wave propagation at regular time intervals (600 time steps). The length of the system was 800 pixels, the width was 250 pixels. The length of the subexcitable area was 600 pixels. The fourth-order Runge–Kutta method and a five-point Laplacian propagator were used (connecting each pixel to its four nearest neighbors). Free boundaries were used in the simulations.

The addition of noise changes the system’s response drastically. Gaussian spatiotemporal noise was added to the excitability parameter  $b$  as follows. The area of propagation was divided into small squares of 100 (10×10) pixels. Within each square, the excitability parameter was assigned a new random value after every 600 time steps. The random values were chosen independently for every square. Within each 600 time steps, the excitability values were maintained constant.

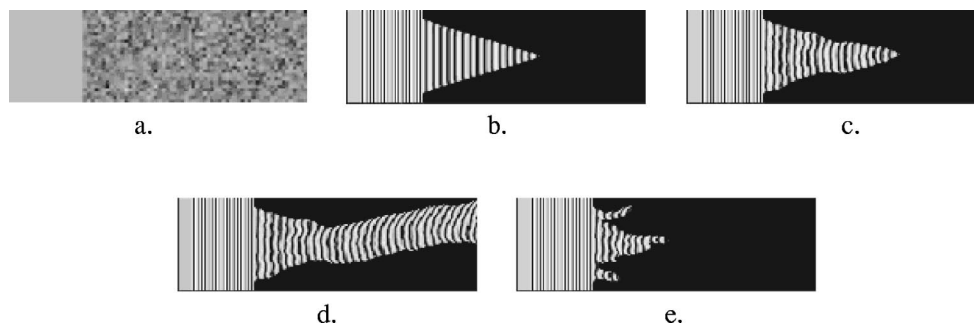


FIG. 4. Sequential images of a wave traveling in a medium governed by the FN equations. (a) The setup: the left-hand side of the medium is excitable, the right-hand side is subexcitable. Observe the noise added to the right-hand side. (b) No noise: the wave has propagated to the border and dies out on the right-hand side. (c) Very weak noise: barely helps if at all. (d) Noise of medium intensity: makes waves propagate indefinitely far. (e) Too strong noise: causes fragmentation of the waves before they can propagate far. The gray scale shades in the images have the following significance: all values are rescaled such that the highest value of  $v$  corresponds to “white” and the lowest value of  $v$  corresponds to “black.”

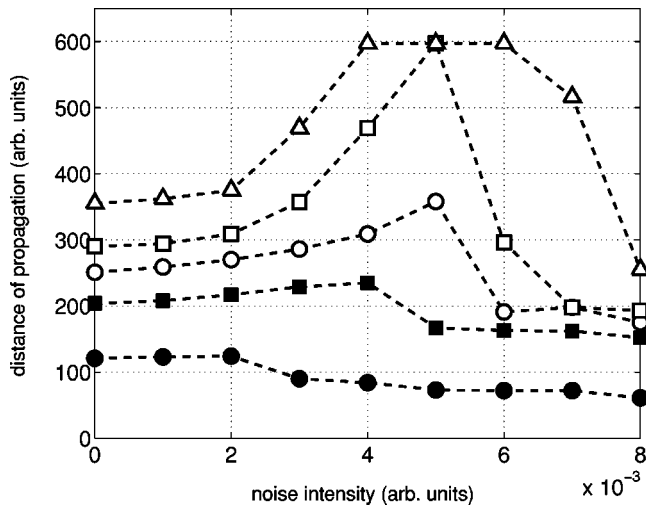


FIG. 5. Propagation length as a function of noise intensity. Filled circles:  $b=0.1960$ ; filled squares:  $b=0.2000$ ; open circles:  $b=0.2010$ ; open squares:  $b=0.2015$ ; open triangles:  $b=0.2020$ . Notice that the propagation length was limited by the dimension of the simulated system. Propagation lengths shown as 600 are actually larger.

The intensity of the noise was defined by its standard deviation  $\sigma$ ,

$$\langle \xi(x,y,t) \cdot \xi(x',y',t') \rangle = \begin{cases} \sigma^2 & \text{for } (x'-x, y'-y, t'-t) \in [0, \Delta_x] \times [0, \Delta_y] \times [0, \Delta_t) \\ 0 & \text{for } (x'-x, y'-y, t'-t) \notin [0, \Delta_x] \times [0, \Delta_y] \times [0, \Delta_t), \end{cases} \quad (3)$$

where  $\Delta_x = \Delta_y = 10$ ,  $\Delta_t = 600$ , and  $\xi(x,y,t)$  is the noise value added to the excitability  $b$  of all 100 pixels in the square that has its lower right corner located at  $(\Delta_x \cdot [x/\Delta_x], \Delta_y \cdot [y/\Delta_y])$ . The square brackets  $[x]$  denote the integer closest to  $x$ , but smaller in value than  $x$ . The reason for choosing a noise with the property (3) is purely biological. The  $10 \times 10$  squares correspond to cells (neurons or astrocytes). There is evidence that the perturbation sweeps unaltered, with constant speed through the cells in the biological situation.<sup>14</sup>

Gradually increasing the noise intensity, we observe that first it helps the waves to propagate farther in the subexcitable area. If the noise intensity is too high, it acts against the propagation by causing wave fragmentation. Wave propagation is optimized for an optimal noise intensity (see Figs. 4 and 5). STSR is thus proven for the two-dimensional FN system.

We define the propagation length as the distance traveled by the wave segment in the subexcitable medium after its ends are cut off. In Fig. 5 the propagation length is shown as a function of the noise intensity, for five different values of the excitability  $b$ . Notice the presence of a peak in both cases, corresponding to the optimal noise intensity.

The computational study of the system governed by the FN equations is important because it can model both neural and glial tissue. Comparing the spiral wave patterns observed

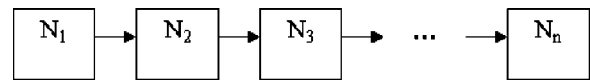


FIG. 6. Neuron chain. The coupling is unidirectional.

in experiments with computer simulations, it has been shown by Jung *et al.* that the glial tissue is a subexcitable medium with self-organized criticality.<sup>24</sup>

### INTEGRATE-AND-FIRE MODEL

Because handling nonlinear differential equations on the computer is a rather complicated task we studied a system of simpler elements that still had the basic features of a neuron. Such a system can be constructed out of IF neurons which have the following parameters: threshold ( $V_T$ ), spike length ( $T_I$ ), recovery period length ( $T_R$ ), memory (or time constant,  $\tau$ ) representing the time for which the neuron “remembers” the incoming charge quanta  $Q_0$ , and excitatory postsynaptic potential per unit time ( $Q_0$ ) arising in the postsynaptic neuron after an action potential arrives to the synapse.<sup>18</sup> Elements with these properties have been connected along a linear chain, as shown in Fig. 6.

All the neurons are passive (they can just transmit a signal, not generate one), and are numbered  $N_1, N_2, N_3, \dots$  (see Fig. 6).

The most important parameter that governs the neurons’ dynamics is their excitability  $e_n(t)$  - an integer number:

- (1) If  $e_n < -T_R$  the neuron is *excitable*;
- (2) if  $-T_R < e_n < 0$  the neuron is in a *recovery period* and its output is equal to zero no matter what is the depolarization on the input;
- (3) if  $0 < e_n$  the neuron is *excited* and it is emitting constant amounts of charge into the synaptic gap.

Every neuron  $N_n$  has a *buffer* (or memory), where it can accumulate the charge quanta emitted by neuron  $n-1$ . If neuron  $n-1$  is excited, the charge in the buffer of neuron  $n$  is increased by  $Q_0$  every time step. We consider the capacitance of the neuron unitary, thus the accumulating charge corresponds to an increasing voltage of equal value. Depending on its excitability  $e_n$ , neuron  $n$  behaves as follows:

- (a) If neuron  $n$  is excitable ( $e_n < -T_R$ ), the voltage  $V_n(t)$  in its buffer is compared to the threshold voltage  $V_T$ . If the voltage  $V_n(t)$  exceeds the threshold  $V_T$ , the excitability  $e_n$  is reset to  $T_I$ , and the voltage in the buffer is reset to 0:  $e_n = T_I$  and  $V_n(t) = 0$  if  $V_n(t) = V_T$ . If  $V_n(t)$  is below the threshold ( $V_n(t) < V_T$ ), the value of the excitability is decreased:  $e_n = e_n - 1$ . If neuron  $n-1$  is in the excited state, an amount of charge  $Q_0$  enters the buffer of neuron  $n$  during each time step.
- (b) If neuron  $n$  is excited ( $0 < e_n$ ), it attempts to inject charge amounts  $Q_0$  into neuron  $n+1$  during each time step, for a time  $T_I$ . This is called *spiking*. Neuron  $n+1$  takes up this charge if it has  $e_{n+1} < -T_R$ . Neuron  $n$  cannot accept charge, independent of the state of

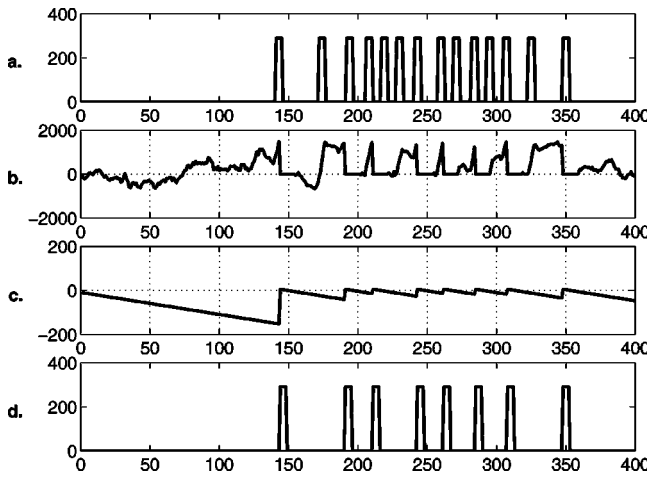


FIG. 7. Propagation of a burst of spikes. (a) The spike burst that arrives into the buffer of neuron  $N_1$ ; (b) the value of the voltage in the buffer (the threshold is  $V_T=1500$ ); (c) the excitability of the neuron; (d) the burst of spikes leaving neuron  $N_1$ .

neuron  $n - 1$ . The buffer stays empty and the excitability is decreased during every time step:  $V_n(t)=0$  and  $e_n = e_n - 1$ .

- (c) If neuron  $n$  is in the recovery period, it does not accept charge from neuron  $n - 1$ , independent of  $e_{n-1}$ . The buffer is kept empty and the excitability decreases with each time step:  $V_n(t)=0$  and  $e_n = e_n - 1$ . This state lasts for a time  $T_R$ .

In addition to the described dynamics, a Gaussian noise term  $\xi_n(t)$  is added to the buffer of the  $n$ th neuron at every time step, with the property

$$\langle \xi_n(t) \cdot \xi_m(t') \rangle = \begin{cases} \sigma^2 & \text{for } m = n \text{ and } t = t' \\ 0 & \text{for } m \neq n \text{ or } t \neq t'. \end{cases} \quad (4)$$

The intensity of this noise term is given by its standard deviation  $\sigma$ .

The neuron model presented here is similar in its nature to the IF model of neuroscience (the buffer in fact integrates the incoming charge over a time interval  $\tau$ ). This model is, however, even more simplified; while the usual definition of the time constant corresponds to an exponential decay, here the decay has the form of a step-function. The neuron *completely* “remembers” any amount of charge that entered its buffer within the last  $\tau$  time steps,

$$Q(t) = Q_0(t) \cdot e^{-(t/\tau)} \rightarrow Q(t) = Q_0(t) \cdot H(\tau - t), \quad (5)$$

where  $H(\tau - t)$  is the Heaviside step-function.

The neuron chain described above operates as presented in Fig. 7, where the response to an incoming random burst of spikes is shown. Notice that in the absence of incoming spikes, voltage variation in the buffer is a random walk, originating from the integral of the white noise in (4). The voltage in the buffer increases abruptly after a spike is received, and is set to 0 during the outgoing spike and the recovery period. A similar two-dimensional model has been used for the definition of STSR in 1995.<sup>25</sup> The present model has the following new features:

- (i) The spikes fired by the neurons are no longer delta-functions. They are rather square pulses of amplitude  $Q_0$  and of duration  $T_I$ .
- (ii) The neurons have a memory (buffer) that stores all the charge quanta arrived within the last  $\tau$  time steps. The charge quanta are “forgotten” completely if they arrived before  $t - \tau$ .

We feed the above-described system with a periodic series of bursts, generated by threshold-crossing of a noisy sinus function as follows. Gaussian white noise was added to a sinus function. The threshold was set above the amplitude of the sinus function and a spike was generated every time the noisy sinus function crossed the threshold in the upwards direction. Two spikes never followed each other less than  $\tau$  apart.

If  $Q_0$  exceeds a *critical value*, the perturbation propagates with no loss along the chain. All neurons will generate the same series of spikes, with some time delay. For small  $Q_0$ , the perturbation is not propagated farther than neuron 1. For subcritical values of  $Q_0$ , close to the critical value, there can be a few neurons that propagate spikes, depending on the value of the time constant  $\tau$ . By adding Gaussian white noise to each of the synapses, the propagation of the input can be extended along the chain even if  $Q_0$  is subcritical. This noise can arise biologically from the neuron itself or from spikes generated by other neurons. It is an internal noise in the sense that it arises inside the organism during information processing.

The system is set up such that noise is necessary for propagation at any “synapse” ( $Q_0$  is subcritical). This is realized by adjusting  $Q_0$ , and keeping the intensity of the noise equal to 0. The signal transmission quality along the chain is defined as the signal to noise ratio at the basic frequency of the sinus function,

$$\text{SNR} = \frac{S - N}{N}, \quad (6)$$

where  $S$  and  $N$  are the signal power and the noise power at the basic frequency, respectively. With the help of this quantity it is possible to study the signal propagation along the neuron chain.

First, the input is a periodic series of spike bursts, and these bursts follow more or less the peaks of the sinus function. The neurons located farther from the input will tend to fire when the previous neuron fired. As the spike series propagates farther along the chain, the resemblance with the input becomes weaker and weaker (see Fig. 8). Although the noise we add to  $Q_0$  at the synapses helps the input ( $N_0$ ) to extend its effect over to neurons located farther and farther, it also causes the SNR to decrease along the chain by scattering and loss of spikes.

We define the “propagation length” as the number of the neuron where SNR becomes less than 1.5 for the first time. In Fig. 9, the value of the SNR is shown as a function of the distance from the input for three different noise intensities. In Fig. 10 the dependence of the propagation length on the noise intensity can be seen. Notice that the largest value of the propagation length is obtained for an intermediary noise intensity.

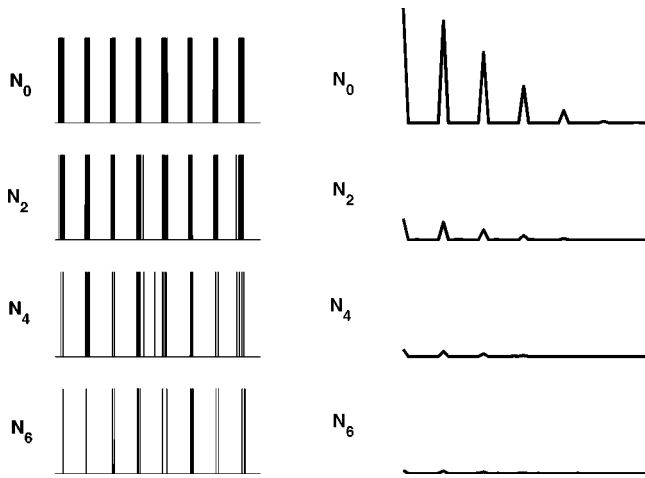


FIG. 8. Spike propagation along the chain. The spike series is shown at the input ( $N_0$ ) and neurons  $N_2$ ,  $N_4$ ,  $N_6$ , on the left. The corresponding power spectra are shown on the right. Notice that the periodicity of the spike series is destroyed by randomization and loss of spikes as it propagates down the chain.

Although the SNR decays with distance along the chain of neurons, according to Fig. 10 there is an optimal noise intensity (approximately 70), for which the signal propagates the farthest. Therefore this simple model shows the phenomenon of STSR. The shape of the STSR curve depends on  $Q_0$ , that is, for higher  $Q_0$  the peak becomes higher and its location moves toward zero noise intensity. For supercritical  $Q_0$ , there is no peak, just a simple decay.

The analogy between the realization of STSR within the present (IF) and the previous (FN) model is noticeable. In both cases the propagation length reaches a maximum for an optimal noise intensity, provided the system is in the subcritical regime of operation.

One of the subtleties that must be noted is that signal transmission strongly depends on the filling factor of the spike series at the entrance. The filling factor can be defined

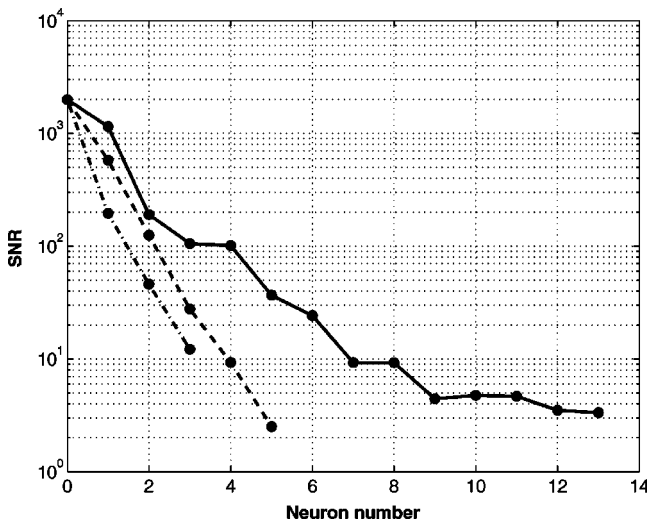


FIG. 9. The decay of SNR along the chain for different noise intensities (the vertical axis has logarithmic scale). The noise intensities were: 10 (dashed line), 60 (solid line), 150 (dashed-dotted line). Notice that the signal propagation is optimal for a noise intensity equal to 60.

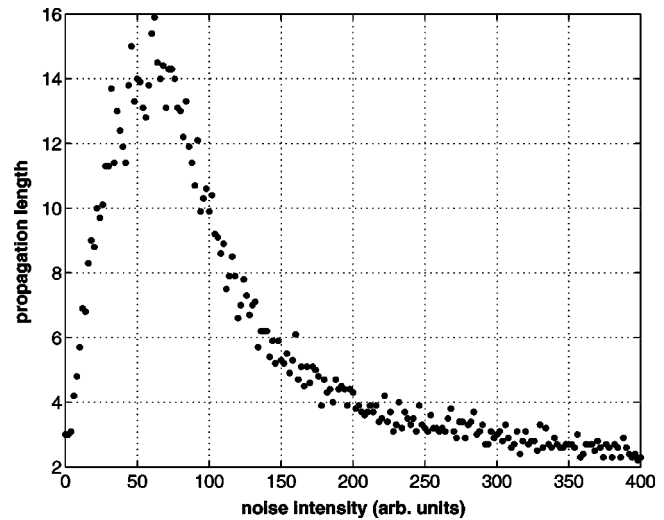


FIG. 10. Propagation length as function of noise intensity. The parameters used were  $V_T=1500$ ,  $T_I=5$ ,  $T_R=5$ ,  $\tau=30$ ,  $Q_0=290$  (300 is the critical value).

as the mean duration of a burst divided by the period of the sinus function used to generate the bursts. According to Ref. 26 the filling factor is what determines the degree to which a stochastic resonator can improve the SNR. For low values of the filling factor there is good transmission, for high values the transmission becomes worse. This point seems to be of crucial importance, since as the filling factor approaches 0.5, the propagation length approaches 0. Based on the above-mentioned reference, the conditions for optimal wave propagation can be determined; at the entrance there must be a perfectly periodic impulse train with low filling factor; the buffer of the neurons has to be very small and  $Q_0$  close to the threshold. Indeed, with such setup we obtained propagation lengths in the range of hundreds of neurons away from the input.

### CONCLUSIONS AND OPEN QUESTIONS

The general conclusion is that STSR is a basic feature of both neural model systems that we studied. In both models, there was an optimal noise intensity which maximized signal transmission. The explanation lies in the common feature of the two models: both are a network of interconnected non-linear (threshold) elements.

The question is whether the same phenomenon happens in reality. Or, in other words, does nature take advantage of STSR (or SR) to propagate signals more efficiently? Is it possible that living organisms use STSR and SR, but they have tuned their noise (and many other parameters) through adaptation and millions of years of evolution to the optimal value?

Despite the fact that SR has been found experimentally in sensory neurons and external noise,<sup>27-29</sup> SR effects due to internal noise are very difficult to observe in living neural systems,<sup>27,30,31</sup> because the tuning of the internal noise intensity causes the cell's parameters to change drastically.

Therefore there seems to be no direct way of proving the existence of STSR (or SR) in biological systems by using

their internal noise. It is questionable whether or not internal noise plays a constructive role in biology. In order to answer this question we need to turn to indirect ways of study. Hence the next question is: Even if it is not possible to “reproduce” SR in biological systems by tuning their internal noise, can we simulate well-known biological (or medical) phenomena by using noisy subexcitable systems? Spiral waves involve periodic, simultaneous activation of distant elements of the neural network, so one can try to make a connection to evoked potentials, EEG signals,<sup>32</sup> etc. An attempt in this direction was made in Ref. 33.

The present paper contains only numerical findings. An important open question is to find a theoretical explanation of the observed phenomena. Experiments confirming our results are also desired. If the existence of STSR in neural systems is proven experimentally, it might become possible to use noise to help patients suffering of synapse disease.

## ACKNOWLEDGMENTS

We are grateful to Sándor Kádár, Jichang Wang, and Kenneth Showalter for helpful discussions and the computer software (developed at the West Virginia University) to solve 2D nonlinear diffusion equations and visualize the solutions. We thank Lon Wilkens, Alexander Neiman, and Eugene Mihaliuk for useful discussions and advice. The research was supported by the Graduate School at the University of Missouri, St. Louis, the U. S. Office of Naval Research, and the Natural Science Research Council (NFR), Sweden.

<sup>1</sup>R. Benzi, A. Sutera, and A. Vulpiani, *J. Phys. A* **14**, L453–457 (1981).

<sup>2</sup>C. Presilla, F. Marchesoni, and L. Gammaitoni, *Phys. Rev. A* **40**, 2105–2113 (1989).

<sup>3</sup>L. Gammaitoni, E. Menichella-Saetta, S. Santucci, F. Marchesoni, and C. Presilla, *Phys. Rev. A* **40**, 2114–2119 (1989).

<sup>4</sup>Z. Gingl, L. B. Kiss, and F. Moss, *Europhys. Lett.* **29**, 191–196 (1995).

<sup>5</sup>F. Moss, in *An Introduction to Some Contemporary Problems in Statistical Physics*, edited by G. H. Weiss (SIAM, Philadelphia, 1994), pp. 205–248.

<sup>6</sup>L. Gammaitoni, P. Hänggi, P. Jung, and F. Marchesoni, *Rev. Mod. Phys.* **70**, 223–287 (1998).

<sup>7</sup>L. B. Kish, G. P. Harmer, and D. Abbott, *Fluct. Noise Lett.* **1**, 13–19 (2001).

<sup>8</sup>S. Kádár, J. Wang, and K. Showalter, *Nature (London)* **391**, 770–772 (1998).

<sup>9</sup>P. Jung, A. Cornell-Bell, F. Moss, S. Kádár, and K. Showalter, *Chaos* **8**, 567–575 (1998).

<sup>10</sup>A. S. Mikhailov, *Foundations of Synergetics I. Distributed Active Systems*, Synergetics Series **51** (Springer, Berlin, 1991), second revised edition, 1994.

<sup>11</sup>A. S. Mikhailov and A. Yu. Loskutov, *Foundations of Synergetics II. Chaos and Noise*, Synergetics Series **52** (Springer, Berlin, 1991), second revised and enlarged edition, 1996.

<sup>12</sup>A. N. Zaikin and A. M. Zhabotinsky, *Nature (London)* **225**, 535–537 (1970).

<sup>13</sup>A. Guderian, K. P. Dechert, and F. W. Schneider, *J. Phys. Chem.* **100**, 5388–5392 (1996).

<sup>14</sup>A. H. Cornell-Bell, S. M. Finkbeiner, M. S. Cooper, and S. J. Smith, *Science* **247**, 470–473 (1990).

<sup>15</sup>A. T. Winfree, *Chaos* **1**, 303–334 (1991).

<sup>16</sup>B. G. Farley, in *Computers in Biomedical Research*, edited by R. W. Stacy and B. D. Waxman (Academic, New York, 1965).

<sup>17</sup>P. Andersen and S. Andersson, *Physiological Basis of the Alphas Rhythm*, APLETON-CENTURY-CROFTS (Meredith, New York, 1968), pp. 198–201.

<sup>18</sup>J. E. Dowling, *Neurons and Networks: An Introduction to Neuroscience* (The Belknap Press of Harvard University Press, Cambridge, MA, 1992).

<sup>19</sup>J. Wang, S. Kádár, P. Jung, and K. Showalter, *Phys. Rev. Lett.* **82**, 855–858 (1999).

<sup>20</sup>J. J. Collins, C. C. Chow, and T. T. Imhoff, *Phys. Rev. E* **52**, R3321–R3324 (1995).

<sup>21</sup>F. Chapeau-Blondeau, X. Godivier, and N. Chambet, *Phys. Rev. E* **53**, 1273–1275 (1996).

<sup>22</sup>R. FitzHugh, *Biophys. J.* **1**, 445–466 (1961).

<sup>23</sup>J. S. Nagumo, S. Arimoto, and S. Yoshizawa, *Proc. IRE* **50**, 2061–2070 (1962).

<sup>24</sup>P. Jung, A. Cornell-Bell, K. Madden, and F. Moss, *J. Neurophysiol.* **70**, 1098–1101 (1998).

<sup>25</sup>P. Jung and G. Mayer-Kress, *Phys. Rev. Lett.* **74**, 2130–2133 (1995).

<sup>26</sup>K. Loerincz, Z. Gingl, and L. B. Kiss, *Phys. Lett. A* **224**, 63–67 (1996).

<sup>27</sup>E. Pantazelou, C. Dames, and F. Moss, *Int. J. Bifurcation Chaos Appl. Sci. Eng.* **8**, 101–108 (1995).

<sup>28</sup>J. E. Levin and J. P. Miller, *Nature (London)* **380**, 165–168 (1996).

<sup>29</sup>B. J. Gluckman, T. I. Netoff, E. J. Neel, W. L. Ditto, M. L. Spano, and S. J. Schiff, *Phys. Rev. Lett.* **77**, 4098–4101 (1996).

<sup>30</sup>F. Y. Chiou-Tan, K. N. Magee, L. R. Robinson, M. R. Nelson, S. S. Tuel, T. A. Krouskop, and F. Moss, *Int. J. Bifurcation Chaos Appl. Sci. Eng.* **6**, 1389–1396 (1996).

<sup>31</sup>X. Pei, L. Wilkens, and F. Moss, *J. Neurophysiol.* **76**, 3002–3011 (1996).

<sup>32</sup>J. A. Hobson, *Sleep* (Scientific American Library, distributed by W. H. Freeman, New York, 1995).

<sup>33</sup>G. Balázsi and L. B. Kish, *Phys. Lett. A* **265**, 304–316 (2000).